Vol. **110** (2006) *ACTA PHYSICA POLONICA A* No. 3

Proceedings of the XXXV International School of Semiconducting Compounds, Jaszowiec 2006

III-Nitride Nanostructures for Infrared Optoelectronics

E. Monroy[a,*], F. Guillot[a], S. Leconte[a], E. Bellet-Amalric[a], L. Nevou[b], L. Doyennette[b], M. Tchernycheva[b], F.H. Julien[b], E. Baumann[c], F. Giorgetta[c], D. Hofstetter[c] and Le Si Dang[d]

[a]CEA-Grenoble, DRFMC/SP2M/PSC
17 rue des Martyrs, 38054 Grenoble, France
[b]Institut d'Electronique Fondamentale, Université Paris-Sud
91405 Orsay, France
[c]University of Neuchâtel, 2000 Neuchâtel, Switzerland
[d]Laboratoire de Spectrométrie Physique, Université Joseph Fourier
38402 Saint Martin d'Hères, France

Thanks to their large conduction band offset (~ 1.8 eV for the GaN/AlN system) and subpicosecond intersubband scattering rates, III-nitride heterostructures in the form of quantum wells or quantum dots are excellent candidates for high-speed unipolar devices operating at optical-fiber telecommunication wavelengths, and relying on the quantum confinement of electrons. In this work, we present the plasma-assisted molecular-beam epitaxial growth of quantum well infrared photodetector structures. The growth of Si-doped GaN/AlN multiple quantum well structures is optimized by controlling substrate temperature, metal excess and growth interruptions. Structural characterization confirms a reduction of the interface roughness to the monolayer scale. *P*-polarized intersubband absorption peaks covering the $1.33-1.91$ μm wavelength range are measured on samples with quantum well thickness varying from 1 to 2.5 nm. Complete intersubband photodetectors have been grown on conductive AlGaN claddings, the Al mole fraction of the cladding matching the average Al content of the active region. Photovoltage measurements reveal a narrow ($\sim$ 90 meV) detection peak at 1.39 μm at room temperature.

PACS numbers: 73.21.Fg, 78.67.De, 85.60.Gz, 85.35.Be, 81.15.Hi, 81.07.St

*corresponding author; e-mail: eva.monroy@cea.fr

1. Introduction

III-nitride semiconductors (GaN, AlN, InN) are currently the materials of choice for optoelectronic devices in the green to UV spectral region. Furthermore, there is a worldwide effort for the development of nitride electronics for high--power/temperature radio-frequency applications. The outstanding physical and chemical stability of nitride semiconductors enable them to operate in harsh environments, and their bio-compatibility and their huge piezoelectric constants render them suitable for the fabrication of chemical sensors and bio-sensors. Moreover, nitride semiconductors are the most "environment-friendly" technology available in the market.

A new prospect for application of III nitrides emerged in the last years: the development of unipolar intersubband (ISB) devices for optoelectronics in the near-infrared. The operating principles of ISB devices have been validated at mid- and far-infrared (IR) wavelengths using materials such as GaAs/AlGaAs or InGaAs/AlInAs-on-InP [1, 2]. Devices such as quantum well infrared photodetectors (QWIP), quantum dot infrared photodetectors (QDIP), electro-optical modulators or quantum cascade lasers have been demonstrated. Thanks to their large conduction band offset ($\sim$ 2 eV for the GaN/AlN system) and subpicosecond ISB scattering rates, III-nitride heterostructures in the form of quantum wells (QWs) or quantum dots (QDs) are excellent candidates for high-speed unipolar devices operating at optical-fiber telecommunication wavelengths, and relying on the quantum confinement of electrons.

Existing semiconductor technologies in the 1.3$-$1.55 μm range are dominated by interband devices using In-GaAs(P)-on-InP. Nitride ISB devices offer advantages such as wavelength tunability, high speed, high-power handling, and material hardness. Furthermore, ISB absorption recovery times are extremely short in III-nitrides ($\sim$ 150$-$400 fs) due to enhanced electron–phonon interaction [3]. In addition, the dielectric constant of nitride semiconductors is about a factor of two smaller than that of InGaAs(P)/InP materials. This opens the way to devices operating in the 0.1–1 Tbit/s bit-rate regime.

Due to the rather large electron effective mass of GaN, layers as thin as 1–1.5 nm are required to achieve narrow ISB absorptions at 1.3$-$1.55 μm. Plasma-assisted molecular beam epitaxy (PAMBE) is the most suitable growth technique for this application due to the low growth temperature, which hinders GaN–AlN interdiffusion. Furthermore, *in situ* monitorization of the surface morphology by reflection high energy electron diffraction (RHEED) makes possible to control the growth at the atomic layer scale. Room temperature ISB absorption at $\lambda \approx$ 1.3$-$1.55 has been demonstrated in both QW [4–8] and QD superlattices [9–11], and several prototypes of ISB detectors [12–15] and electro-optical modulators [16] have recently been reported. These developments are possible thanks to improved deposition techniques for Al(Ga)N/GaN layers and superlattices [17–19]. Furthermore, high-resolution transmission electron microscopy (HRTEM) shows

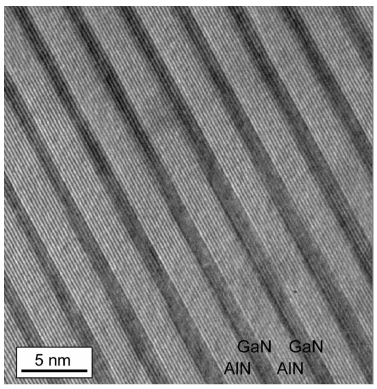

Fig. 1. HRTEM image of the active region of a QWIP structure.

homogeneous quantum wells with an interface roughness of ∼1 ML (see Fig. 1 and interface analysis in Ref. [18]).

In this work we review our progress towards the fabrication of nitride-based ISB devices operating in the 1.3–1.55 μm range. We present the optimization of plasma-assisted MBE growth of QWIP structures, from the Si-doped GaN/AlN short-period superlattice of the active region to the integration of the final device. Finally we discuss the structural, optical, and electrical characterization of a complete QWIP.

2. GaN/AlN multiple-quantum-well structures

AlGaN/AlN/GaN multiple-quantum-well (MQW) structures have been synthesized by PAMBE on *c*-sapphire. The growth rate was fixed at ~ 0.3 monolayers per second (ML/s) by the flux of active nitrogen. The growth optimization of GaN/AlN interfaces requires determining conditions compatible for GaN and AlN growth, GaN being the most restrictive material due to its lower decomposition temperature. Best GaN structural quality is achieved by deposition under Ga-rich conditions with 2 monolayers (ML) of Ga-excess segregating at the growth front [20]. The quality of the GaN/AlN heterostructures was found to be particularly sensitive to the Ga/N ratio. The strain fluctuations induced by Si doping and by the presence of the AlN barriers favor the formation of V-shaped pits, even in layers grown in the regime of 2 ML Ga-excess [21, 22]. The suppression of these defects has been achieved by an enhancement of the Ga-flux so that growth is performed at the limit of Ga-accumulation.

In the case of AlN, growth under Al-rich conditions is required to achieve two-dimensional growth. However, Al is not desorbed from the surface at the standard growth temperatures for GaN. Therefore, to prevent Al accumulation at the surface, it is necessary to perform periodic growth interruptions under nitrogen. An alternative approach to prevent growth interruptions consists on using Ga as a surfactant for the growth of AlN, with the Al flux corresponding to

the Al/N stoichiometry and using an additional Ga flux to stabilize the surface. Since the Al–N binding energy is much higher than the Ga–N binding energy, Ga segregates on the surface and it is not incorporated into the AlN layer. Best interface absorption, attributed to transition from the first to the second electronic levels in the QW ($e_1 \rightarrow e_2$), while no absorption was found for s-polarized light within experimental accuracy. The spectra present a Lorentzian shape, indicative of homogeneous broadening of the absorption. The linewidth of the absorption

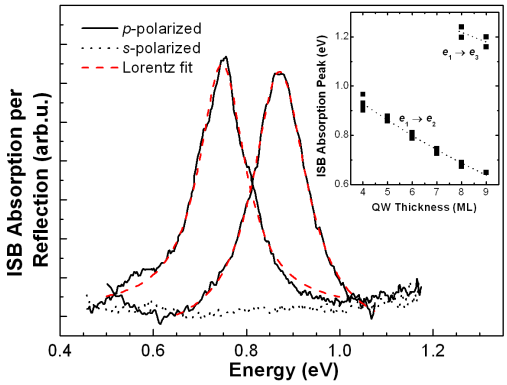

Fig. 2. Room-temperature ISB absorption spectra of AlN/GaN MQW structures for p-polarized and s-polarized light. The QW thicknesses are equal to 5 ML and 7 ML. Dashed lines present Lorentzian fits of the spectra. Inset: Variation of the $e_1 \rightarrow e_2$ and $e_1 \rightarrow e_3$ ISB absorption peaks as a function of the QW width, for samples doped in the QWs at 5×10^{19} cm^{-3}.

remains in the 70–120 meV range for QWs doped at 5×10^{19} cm^{-2}, and the ISB absorption efficiency per reflection attains 3–5%. A record bandwidth of ~ 40 meV has been achieved in non-intentionally doped structures. As displayed in the inset of Fig. 2, the ISB absorption peak can be tuned in the 1.33 to 1.91 μm wavelength range by changing the QW thickness from 4 ML to 10 ML. For larger QWs, the $e_1 \rightarrow e_3$ transition is observed [8]. This transition is allowed in nitride QWs because of the presence of strong internal electric field in the well that breaks the symmetry of the potential. A detailed modeling of ISB absorption of these samples is presented in Ref. [8].

3. QWIP structures

We have fabricated complete QWIP structures consisting of 40 periods of 1.0 nm thick Si-doped GaN QWs with 2.0 nm thick AlN barriers, grown on a 250 nm thick Si-doped $Al_{0.65}Ga_{0.35}N$ contact layer. Substrates consisted of 1 μm thick AlN-on-sapphire templates. The doping level in the GaN QWs was 1×10^{19} cm^{-3}. On top of the active region, we deposited a Si-doped $Al_{0.65}Ga_{0.35}N$ cap layer, with a thickness of 5 nm.

The structural quality of the QWIP structure has been assessed by atomic force microscopy (AFM) and high-resolution X-ray diffraction (HRXRD). The rms surface roughness remains about 1.7 nm on an area of 5×5 μm^2, atomic terraces being observable on the sample surface. Figure 3 shows the $(\theta{-}2\theta)$-scan of the (0002) X-ray reflection, displaying superlattice satellite peaks up to the second order, which confirm an average period of 2.93 nm. From simulations of this scan (also presented in Fig. 3), and from the (10–15) reciprocal space map, we verified that the average Al mole fraction of the claddings matches the average Al content of the MQW structure, and that the whole structure is strained on the AlN buffer layer.

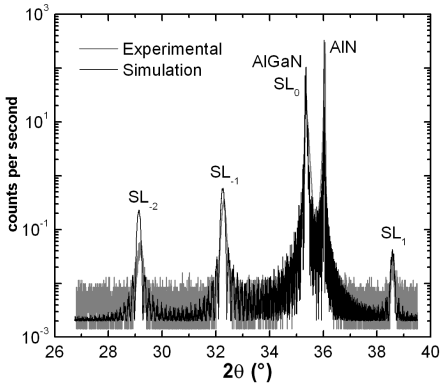

Fig. 3. HRXRD $\theta - 2\theta$ scan of the (0002) reflection of a QWIP structure. Superlattice (SL) satellite peaks up to the second order are clearly visible, whereas the SL zero-order reflection peak (SL_0) overlaps with the $Al_{0.65}Ga_{0.35}N$ reflection. An average period of 2.93 nm is obtained from the inter-satellite distance. The simulation was performed using the program X'Pert Epitaxy 40 from Phillips Analytical, assuming that the structure is fully strained on the AlN buffer.

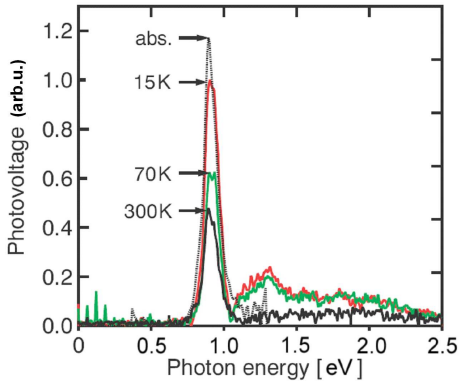

Fig. 4. Temperature-dependent photovoltage measurements for p-polarized light. The absorbance spectrum is shown as a dotted line for comparison.

To fabricate a QWIP, the above-described sample was polished in a standard multipass geometry with a mirror-like back and two parallel 45° wedges. Two Cr/Au (10/400 nm) ohmic contacts were deposited on the sample surface, separated by 3 mm. In between, a large stripe of the same contact metals was evaporated on top of a 50 nm thick SiO_2 layer deposited on the semiconductor surface. Figure 4 presents the characterization of this device as a photovoltaic ISB photodetector. In this experiment, the sample was illuminated by the white light source of the Fourier spectrometer. The Schottky contact leads to a band bending at the sample surface, depleting several periods of the active region. Illumination results in a photovoltage, which can be observed up to room temperature, as shown in Fig. 4. A good agreement between the photovoltage signal and the absorbance peak is evident. The photovoltage at 10 K peaks at 0.915 eV (1.39 μm), and has a FWHM of 90 meV. This extremely narrow peak confirms the good structural material quality.

4. Conclusions

Plasma-assisted molecular beam epitaxy has been adapted for the growth of AlGaN/AlN/GaN quantum well infrared photodectors operating in the optical--fiber telecommunication spectral range. Si-doped GaN/AlN multiple quantum well structures with interface roughness at the monolayer scale were successfully synthesized. These structures present ISB absorption peaks that can be tuned in the 1.33−1.91 μm wavelength range by varying the QW thickness from 1 to 2.5 nm. To prevent partial depletion of the QWs due to the internal electric field, we have developed highly-conductive Si-doped AlGaN cladding layers using In as a surfactant during growth. Complete ISB photovoltaic detectors have been fabricated. Temperature dependent photovoltage measurements reveal a narrow ($\sim$ 90 meV) detection peak at 1.39 μm.

Acknowledgments

This work is supported by the 6th European Framework Program within the project NITWAVE (STREP 004170).

References

[1] J. Faist, F. Capasso, D.L. Sivco, C. Sirtori, A.L. Hutchinson, A.Y. Cho, *Science* **264**, 553 (1994).

[2] B.F. Levine, K.K. Choi, C.G. Bethea, J. Walker, R.J. Malik, *Appl. Phys. Lett.* **50**, 1092 (1987).

[3] N. Iizuka, K. Kaneko, N. Suzuki, *Appl. Phys. Lett.* **81**, 1803 (2002).

[4] C. Gmachl, H.M. Ng, A.Y. Cho, *Appl. Phys. Lett.* **79**, 1590 (2001).

[5] N. Iizuka, K. Kaneko, N. Suzuki, *Appl. Phys. Lett.* **81**, 1803 (2002).

[6] K. Kishino, A. Kikuchi, H. Kanazawa, T. Tachibana, *Appl. Phys. Lett.* **81**, 1234 (2002).

[7] A. Helman, M. Tchernycheva, A. Lusson, E. Warde, F.H. Julien, Kh. Moumanis, G. Fishman, E. Monroy, B. Daudin, Le Si Dang, E. Bellet-Amalric, D. Jalabert, *Appl. Phys. Lett.* **83**, 5196 (2003).

[8] M. Tchernycheva, L. Nevou, L. Doyennette, F.H. Julien, E. Warde, F. Guillot, E. Monroy, E. Bellet-Amalric, T. Remmele, M. Albrecht, *Phys. Rev. B* **73**, 125347 (2006).

[9] K. Moumanis, A. Helman, F. Fossard, M. Tchernycheva, A. Lusson, F.H. Julien, B. Damilano, N. Grandjean, J. Massies, *Appl. Phys. Lett.* **82**, 868 (2003).

[10] M. Tchernycheva, L. Nevou, L. Doyennette, A. Helman, R. Colombelli, F.H. Julien, F. Guillot, E. Monroy, T. Shibata, M. Tanaka, *Appl. Phys. Lett.* **87**, 101912 (2005).

[11] F. Guillot, E. Bellet-Amalric, E. Monroy, M. Tchernycheva, L. Nevou, L. Doyennette, F.H. Julien, Le Si Dang, T. Remmele, M. Albrecht, T. Shibata, M. Tanaka, *J. Appl. Phys* **100**, 044326 (2006).

[12] D. Hofstetter, S.-S. Schad, H. Wu, W.J. Schaff, L.F. Eastman, *Appl. Phys. Lett.* **83**, 572 (2003).

[13] D. Hofstetter, E. Baumann, F.R. Giorgetta, M. Graf, M. Maier, F. Guillot, E. Bellet-Amalric, E. Monroy, *Appl. Phys. Lett.* **88**, 121112 (2006).

[14] L. Doyennette, L. Nevou, M. Tchernycheva, A. Lupu, F. Guillot, E. Monroy, R. Colombelli, F.H. Julien, *Electron. Lett.* **41**, 1077 (2005).

[15] A. Vardi, N. Akopian, G. Bahir, L. Doyennette, M. Tchernycheva, L. Nevou, F.H. Julien, F. Guillot, E. Monroy, *Appl. Phys. Lett.* **88**, 143101 (2006).

[16] E. Baumann, F.R. Giorgetta, D. Hofstetter, S. Leconte, F. Guillot, E. Bellet--Amalric, E. Monroy, submitted to *Appl. Phys. Lett.*

[17] E. Monroy, B. Daudin, E. Bellet-Amalric, N. Gogneau, D. Jalabert, F. Enjalbert, J. Brault, J. Barjon, Le Si Dang, *J. Appl. Phys.* **93**, 1550 (2003).

[18] E. Sarigiannidou, E. Monroy, N. Gogneau, G. Radtke, P. Bayle-Guillemaud, E. Bellet-Amalric, B. Daudin, J.L. Rouvière, *Semicond. Sci. Technol.* **21**, 912 (2006).

[19] E. Monroy, F. Guillot, B. Gayral, E. Bellet-Amalric, D. Jalabert, J.-M. Gérard, Le Si Dang, M. Tchernycheva, F.H. Julien, *J. Appl. Phys.* **99**, 093513 (2006).

[20] C. Adelmann, J. Brault, G. Mula, B. Daudin, L. Lymperakis, J. Neugebauer, *Phys. Rev. B* **67**, 165419 (2003).

[21] T. Nakamura, S. Mochizuki, S. Terao, T. Sano, M. Iwaya, S. Kamiyama, H. Amano, I. Akasaki, *J. Cryst. Growth* **237-239**, 1129 (2002).

[22] M. Hermann, E. Monroy, A. Helman, B. Baur, M. Albrecht, B. Daudin, O. Ambacher, M. Stutzmann, M. Eickhoff, *Phys. Status Solidi C* **1**, 2210 (2004).

[23] N. Gogneau, G. Jalabert, E. Monroy, E. Sarigiannidou, J.-L. Rouvière, T. Shibata, M. Tanaka, J.-M. Gérard, B. Daudin, *J. Appl. Phys.* **96**, 1104 (2004).